Inorg. Chem. **2002**, *41*, 1194–1198

Inorganic Chemistry

Article

Metal Scrambling in the Trinuclear $\{Pt_2Se_2M\}$ (M = Pt, Pd, Au) System Using an Electrospray Mass Spectrometry (ESMS) Directed Synthetic Methodology; Isolation and Crystallographic Characterization of $\{Pt_2(\mu_3\text{-}Se)_2(PPh_3)_4[Pt(cod)]\}\{PF_6\}_2$ and $\{Pt(\mu_3\text{-}Se)_2(PPh_3)_2[Pt(cod)]_2\}\{PF_6\}_2$ (cod = Cyclo-octa-1,5-diene)

Jeremy S. L. Yeo,[†] Jagadese J. Vittal,[†] William Henderson,[‡,*] and T. S. Andy Hor[†,*]

Department of Chemistry, National University of Singapore, 3 Science Drive 3, Singapore 117543, and Department of Chemistry, University of Waikato, Private Bag 3105, Hamilton, New Zealand

Received August 14, 2001

$Pt_2(\mu\text{-}Se)_2(PPh_3)_4$ reacts with $PtCl_2(cod)$ to give $\{Pt_2(\mu_3\text{-}Se)_2(PPh_3)_4[Pt(cod)]\}^{2+}$ and an unexpected cod-rich product that arises from metal scrambling, viz. $\{Pt(\mu_3\text{-}Se)_2(PPh_3)_2[Pt(cod)]_2\}^{2+}$. The formation of these species was detected and followed by electrospray mass spectrometry (ESMS) and subsequently verified by batch synthesis and crystallographic characterization. Other metal-scrambled aggregate products were successfully detected.

Introduction

Metal exchange reactions were first observed in the early 1970s,[1] but systematic studies of this type of reaction were not carried out until recently.[2] "Metal scrambling" involves the interchange of metal sites (usually with their respective coordinated ligands) and should not be confused with "ligand scrambling" (with metal positions intact but ligands interchange), which was elegantly described by Braunstein et al.[3] and other researchers.[4] When metals switch positions by an intermolecular mechanism, especially among heterometallic species, the process is usually undesirable, as it would destroy the mixed-metal formalism and, hence, its functionality. A classical example is homogeneous catalytic activity at a hetero metal−metal bond. Loss of such an entity would seriously jeopardize the catalytic functionality of the system. There are, unfortunately, very few simple and convenient in situ techniques that could help identify such a process or products in solution. The development of such a technique would help design (or avoid) such dynamic multimetallic systems. In this paper, using the $\{Pt_2Se_2M\}$ system as a model, we describe an unprecedented use of electrospray mass spectrometry (ESMS) in capturing metal-scrambled species. This trimetallic system is derived from metalation of $[Pt_2(\mu\text{-}Se)_2(PPh_3)_4]$, **1**, at the two Lewis basic selenide centers. The products were subsequently verified by synthetic isolation and crystallographic analyses. The use of ESMS as a diagnostic technique in following heterometalation of **1** (with Sn(IV)[5] and $[Pt_2(\mu\text{-}S)_2(PPh_3)_4]$;[6] Chart 1) has been described. A related approach in the use of ESMS in studying metal cluster mixtures has been described.[7] Although the

---

* Authors to whom correspondence should be addressed. E-mail: w.henderson@waikato.ac.nz (W.H.); andyhor@nus.edu.sg (T.S.A.H.).

[†] National University of Singapore.

[‡] University of Waikato.

(1) (a) Hsieh, A. T.; Mays, M. J. *J. Organomet. Chem.* **1971**, *26*, 125. (b) Knight, J.; Mays, M. J. *J. Chem. Soc., Dalton Trans.* **1972**, 1022.

(2) (a) Zhang, J.; Zhang, Y.-H.; Chen, X.-N.; Ding, E −R.; Yin, Y.-Q. *Organometallics* **2000**, *19*, 5032. (b) Chen, X.-N.; Zhang, J.; Yin, Y.-Q.; Huang, X.-Y. *Organometallics* **1999**, *18*, 3164. (c) Ding, E.-R.; Yin, Y.-Q.; Sun, J. *Polyhedron* **1997**, *17*, 3067. (d) Song, L.-C.; Shen J.-Y.; Hu, Q.-M.; Huang, X.-Y. *Organometallics* **1995**, *14*, 98. (e) Schach, H. T.; Vahrenkamp, H. *J. Organomet. Chem.* **1990**, *381*, 261. (f) Blumhofer, R.; Fischer, K. *Chem. Ber.* **1986**, *119*, 194. (g) Vahrenkamp, H. *Comments Inorg. Chem.* **1985**, *4*, 253.

(3) (a) Braunstein, P.; Richert, J.-L.; Dusausoy, Y. *J. Chem. Soc., Dalton Trans.* **1990**, 3801. (b) Braunstein, P.; Kervennal J.; Richert, J.-L. *Angew. Chem., Int. Ed. Engl.* **1985**, *24*, 768.

(4) (a) Yeo, J. S. L.; Li, G.; Yip, W.-H.; Henderson, W.; Mak, T. C. W.; Hor, T. S. A. *J. Chem. Soc., Dalton Trans.* **1999**, 435. (b) Bantel, H.; Bernhardt, W.; Powell, A. K.; Vahrenkamp, H. *Chem. Ber.* **1988**, *121*, 1247.

(5) Yeo, J. S. L.; Vittal, J. J.; Henderson, W.; Hor, T. S. A. *J. Chem. Soc., Dalton Trans.* **2001**, 315.

(6) (a) Fong, S.-W. A.; Yap, W. T.; Vittal, J. J.; Oliver, A. G.; Rickard, C. E. F.; Henderson, W.; Hor, T. S. A. *J. Chem. Soc., Dalton Trans.* **2001**, 1986. (b) Fong, S.-W. A.; Vittal, J. J.; Henderson, W.; Hor, T. S. A.; Oliver, A. G.; Rickard, C. E. F. *Chem. Commun.* **2001**, 421.

(7) Dyson, P. J.; Hearley, A. K.; Johnson, B. F. G.; Khimyak, T.; McIndoe, J. S.; Langridge-Smith, P. R. R. *Organometallics* **2001**, *20*, 3970.

10.1021/ic010905t CCC: $22.00

Chart 1

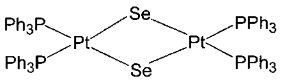

1

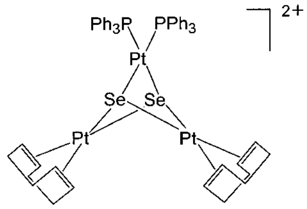

2

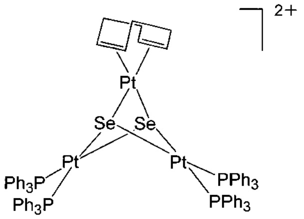

3

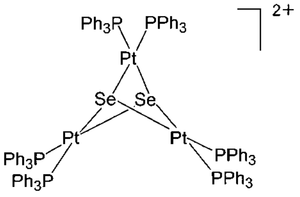

4

sulfide system has been well explored, there is insofar no observable scrambling in all the mixed-metal aggregates we have studied.[6] The chosen model is based on the products from the Lewis base/acid interaction between **1** and $PtCl_2$(cod) (cod = cyclo-octa-1,5-diene). The choice of the same metal (Pt) in the substrate illustrates that this approach can also apply to homonuclear systems. In this work, we shall illustrate the simplicity of this methodology in monitoring this molecular transformation, which turns a complex with one active site (with a [Pt(cod)] moiety) to one that has two such sites. This conversion highlights a rare benefit of metal scrambling in heterometallic synthesis.

Experimental Section

Samples for ESMS analysis were prepared by dissolving **1** and substrate (both 10−100 μg) in 1 mL of MeOH. Electrospray mass spectra were obtained with a VG Platform II mass spectrometer with the methanol mobile phase driven at 0.02 mL min^{-1} using a Thermo Separation products SpectraSystem P1000 LC pump. Samples were injected via a Rheodyne valve fitted with a 10 μL sample loop. The source temperature was 60 °C. The capillary potential tip was 3500 V, with nitrogen used both as a drying and a nebulizing gas. The skimmer cone voltage was usually 5 V when clean parent ions were required and was varied up to 80 V to investigate fragmentation processes. Peaks were assigned from the *m*/*z* values and from the isotope distribution patterns that were simulated using the ISOTOPE program.[8] The *m*/*z* values given are for the most intense peak in the envelope in each case.

Single-crystal data collections were performed on a Bruker AXS SMART diffractometer, equipped with a CCD area detector using Mo Kα radiation (λ = 0.71073 Å). The software SMART[9] was used for collecting frames of data, indexing reflections, and determining lattice parameters, SAINT[9] for integration of intensity of reflections and scaling, SADABS[10] for empirical absorption correction, and SHELXTL[11] for space group and structure determination, refinements, graphics, and structure reporting. The structures were refined by full-matrix least squares on F^2 with anisotropic thermal parameters for non-hydrogen atoms, unless otherwise indicated [$R1 = \sum||F_o| - |F_c||/\sum|F_o|$, and $wR2 = \{\sum[w(F_o^2 - F_c^2)^2]/\sum[w(F_o^2)^2]\}^{1/2}$ (where $w^{-1} = \sigma^2(F_o^2) + (aP)^2 + (bP)$)]. Supporting Information including non-hydrogen and hydrogen atomic coordinates, thermal parameters for the non-hydrogen atoms, and complete tables of bond distances and angles has been deposited at the Cambridge Crystallographic Data Centre (CCDC).

^{1}H and ^{13}C NMR spectra were recorded at 25 °C on a Bruker ACF 300 spectrometer (at 300 and 75.47 MHz, respectively) with tetramethylsilane (TMS) as external reference. The ^{31}P NMR spectra were recorded at 121.39 MHz with 85% H_3PO_4 as external reference. Elemental analyses were performed by the microanalytical laboratory of the Department of Chemistry at the National University of Singapore. Samples have been crushed into fine powder and subjected to vacuum before sending for these analyses.

A modified preparation of $Pt_2(\mu\text{-Se})_2(PPh_3)_4$, **1**, was adapted from our recent report.[5] All reactions were performed under a positive pressure of purified argon unless otherwise stated, and solvents were distilled and degassed before use.

Synthesis of $\{Pt(\mu_3\text{-Se})_2(PPh_3)_2[Pt(cod)]_2\}\{PF_6\}_2$ (2) and $\{Pt_2(\mu_3\text{-Se})_2(PPh_3)_4[Pt(cod)]\}\{PF_6\}_2$ (3). $PtCl_2$(cod) (11.5 mg, 0.0307 mmol) was added to a brown suspension of **1** (47.3 mg, 0.0296 mmol) in MeOH (20 mL). The resulting orange solution was stirred for 3 h, after which excess NH_4PF_6 (10.0 mg, 0.0614 mol) was introduced to give an orange-brown suspension. After the reaction mixture was stirred for 1 h, deionized water (50 mL) was added to induce precipitation. The suspension was filtered and the solid washed successively with 100 mL portions of deionized water and Et_2O and dried under vacuum yielding an orange-brown powder (0.0446 g) containing a mixture of **2** and **3**. Both **2** (0.0246 g, 55% cf. mixture) and **3** (0.0125 g, 28% cf. mixture) were separated from the mixture by recrystallization with CH_2Cl_2−hexane. Found for **2**: C, 35.0; H, 3.1; P, 6.7. Calcd for $C_{52}H_{54}F_{12}Se_2P_4Pt_3$: C, 35.2; H, 3.1; P, 7.0%. $^{31}P\{^1H\}$ NMR ($CDCl_3$): δ_P 13.2 [t (1:4:1), ^1J(P−Pt) = 3300 Hz], −144.1 ppm [heptet, ^1J(P−F) = 713 Hz]. ^{13}C NMR ($CDCl_3$): δ_C 30.8 [m, 8 C (8 C−C on cod)], 131.6 [m, 8 C (8 C=C on cod)], 128.6 and 133.9 ppm [m, 36 C (6 C_6H_5)]. ^{1}H NMR ($CDCl_3$): δ_H 2.52−2.72 [m, 16 H (8 CH_2)], 4.62 [s, 8 H (8 C=CH)], 7.05−7.52 ppm [m, 30 H (6 C_6H_5)]. Found for **3**: C, 43.2; H, 3.1; P, 7.7. Calcd for $C_{80}H_{72}F_{12}Se_2P_6Pt_3$: C, 43.9; H, 3.3; P, 8.5%. $^{31}P\{^1H\}$ NMR ($CDCl_3$): δ_P 14.8 [t (1:4:1), ^1J(P−Pt) = 3300 Hz], −144.0 ppm [heptet, ^1J(P−F) = 713 Hz]. ^{13}C NMR ($CDCl_3$): δ_C 30.2 [m, 4 C (4 C−C on cod)], 131.1 [m, 4 C (4 C=C on cod)], 128.4 and 133.8 ppm [m, 72 C (12 C_6H_5)]. ^{1}H NMR ($CDCl_3$): δ_H 2.45−2.57 [m, 8 H (4 CH_2)], 4.64 [s, 4 H (4 C=CH)], 7.12−7.47 ppm [m, 60 H (12 C_6H_5)].

Suitable single crystals of **2** and **3** for structure determination were obtained by layering a CH_2Cl_2 solution of each compound with hexane.

Compound 2. A suitable crystal of dimensions 0.20 × 0.14 × 0.12 mm^3 was mounted at the end of a glass fiber and cooled to −50 °C for data collection. A total of 27042 reflections were collected in the θ range 1.78°−25.00° ($-16 < h < 18$, $-14 < k < 10$, $-33 < l < 34$).

---

(8) Arnold, L. J. *J. Chem. Educ.* **1992**, *69*, 811.

(9) *SMART & SAINT Software Reference Manuals*, version 4.0; Siemens Energy & Automation, Inc., Analytical Instrumentation: Madison, WI, 1996.

(10) Sheldrick, G. M. *SADABS, a software for empirical absorption correction*; University of Göttingen: Göttingen, Germany, 1993.

(11) Sheldrick, G. M. *SHELXTL*, version 5.03; Siemens Energy & Automation, Inc., Analytical Instrumentation: Madison, WI, 1996.

Table 1. Selected Bond Lengths (Å) and Angles (deg) of Complexes **2** and **3**

$\{Pt(\mu_3\text{-}Se)_2(PPh_3)_2\text{-}[Pt(cod)]_2\}\{PF_6\}_2$ (**2**)		$\{Pt_2(\mu_3\text{-}Se)_2(PPh_3)_4[Pt(cod)]\}\text{-}\{PF_6\}_2$ (**3**)$\cdot 2.5CH_2Cl_2\cdot 3.5H_2O$	
Pt(1)−Se(1)	2.4919(6)	Pt(1)−Se(1)	2.4625(9)
Pt(1)−Se(2)	2.4723(6)	Pt(1)−Se(2)	2.4719(10)
Pt(2)−Se(1)	2.4600(6)	Pt(2)−Se(1)	2.4744(9)
Pt(2)−Se(2)	2.4428(6)	Pt(2)−Se(2)	2.4607(10)
Pt(3)−Se(1)	2.4445(6)	Pt(3)−Se(1)	2.4283(10)
Pt(3)−Se(2)	2.4392(6)	Pt(3)−Se(2)	2.4305(11)
Pt(2)−C(1)	2.207(6)	Pt(3)−C(1)	2.178(10)
Pt(2)−C(2)	2.211(6)	Pt(3)−C(2)	2.195(9)
Pt(2)−C(5)	2.191(6)	Pt(3)−C(5)	2.173(10)
Pt(2)−C(6)	2.212(6)	Pt(3)−C(6)	2.169(10)
Pt(3)−C(9)	2.192(7)		
Pt(3)−C(10)	2.208(7)		
Pt(3)−C(13)	2.195(6)		
Pt(3)−C(14)	2.210(6)		
Pt(1)−Se(1)−Pt(2)	83.479(19)	Pt(1)−Se(1)−Pt(2)	89.79(3)
Pt(1)−Se(2)−Pt(2)	84.246(19)	Pt(1)−Se(2)−Pt(2)	89.89(3)
Pt(1)−Se(1)−Pt(3)	84.847(19)	Pt(1)−Se(1)−Pt(3)	79.79(3)
Pt(1)−Se(2)−Pt(3)	85.38(2)	Pt(1)−Se(2)−Pt(3)	79.56(3)
Pt(2)−Se(1)−Pt(3)	77.293(18)	Pt(2)−Se(1)−Pt(3)	80.20(3)
Pt(2)−Se(2)−Pt(3)	77.716(18)	Pt(2)−Se(2)−Pt(3)	80.43(3)
Se(1)−Pt(1)−Se(2)	80.23(2)	Se(1)−Pt(1)−Se(2)	79.02(3)
Se(1)−Pt(2)−Se(2)	81.44(2)	Se(1)−Pt(2)−Se(2)	79.01(3)
Se(1)−Pt(3)−Se(2)	81.83(2)	Se(1)−Pt(3)−Se(2)	80.50(3)
P(1)−Pt(1)−P(2)	99.50(5)	P(1)−Pt(1)−P(2)	98.62(8)

Table 2. Crystallographic Data for Complexes **2** and **3**

	2	**3**$\cdot 2.5CH_2Cl_2\cdot 3.5H_2O$
formula	$C_{52}H_{54}F_{12}Se_2P_4Pt_3$	$C_{82.5}H_{84}Cl_5F_{12}O_{3.5}Se_2P_6Pt_3$
fw	1774.02	2465.76
cryst syst	monoclinic	monoclinic
space group	$P2(1)/c$	$P2(1)/n$
a/Å	15.8939(2)	17.693(3)
b/Å	11.8889(1)	23.952(4)
c/Å	29.2574(1)	21.129(4)
α/deg	90	90
β/deg	97.456(1)	91.272(5)
γ/deg	90	90
V/Å^3	5481.76(9)	8952(3)
Z	4	4
d/gcm^{-3}	2.150	1.830
μ/mm^{-1}	9.158	5.818
T/K	223(2)	223(2)
no. unique reflns	9562	15750
no. obsd reflns $[I > 2\sigma(I)]$, (R_{int})	7788 (0.0314)	10184 (0.0655)
$R\ [I > 2\sigma(I)]$	0.0286	0.0482
$wR_2\ [I > 2\sigma(I)]$	0.0561	0.1163

Compound 3$\cdot$2.5CH$_2$Cl$_2\cdot$3.5H$_2$O. A suitable crystal of dimensions 0.44 × 0.20 × 0.10 mm^3 was mounted at the end of a glass fiber and cooled to −50 °C for data collection. A total of 51943 reflections were collected in the θ range 1.70°−25.00° ($-20 < h < 21$, $-28 < k < 28$, $-25 < l < 20$). There are 2.5 CH_2Cl_2 and 3.5 H_2O solvates present in the asymmetric unit, and they are highly disordered. The electron densities were assigned on the basis of the solvents used for growing the data crystal and the geometric parameters observed. The occupancies in these disordered solvates were assigned on the basis of the relative electron densities found in the Fourier difference map, and they were not refined. In one CH_2Cl_2, two orientations of the Cl atoms were modeled with occupancies of 0.5 and 0.5. In another place, two independent CH_2Cl_2 solvates were found with occupancies of 0.7 and 0.3. Common isotropic thermal parameters were refined for the non-hydrogen atoms in each model. All the C−Cl and Cl···Cl distances were fixed at 1.60 and 2.56 Å, respectively. The electron densities near the (110) plane were assigned to oxygen atoms of the disordered water molecules, and seven such O atoms were assigned with an occupancy of 0.5 each.

Results and Discussion

We have used ESMS to follow the metalation of **1** with a range of largely platinum metal substrates, viz. $PtCl_2(cod)$,[12] *cis*-$PtCl_2[P(OPh)_3]_2$,[13] *cis*-$PtCl_2(PMe_3)_2$,[14] $PdCl_2(cod)$,[15] $PdCl_2(phen)$ (phen = 1,10-phenanthroline),[16] $[RhCl_2Cp^*]_2$ ($Cp^* = \eta^5\text{-}C_5Me_5$),[17] and $AuCl_2$(2-bzpy) (2-bzpy = *C*,*N*-2-benzylpyridyl),[18] and to identify their products. Besides the expected chloride displacement to form $[\mathbf{1}(\text{substrate} - x\text{Cl})]^{x+}$ ($x = 1, 2$), the species $[PtSe_2(PPh_3)_2(\text{substrates} - 2Cl)_2]^{2+}\}$ were surprisingly detected. The $[Pt_3Se_2(cod)]$ system was chosen for detailed analysis. Analysis of a reaction mixture of **1** and $PtCl_2(cod)$ (in MeOH) at a low cone voltage (20 V) gave products that could be formulated as $\{Pt(\mu_3\text{-}Se)_2(PPh_3)_2[Pt(cod)]_2\}^{2+}$ (**2**), the expected $\{Pt_2(\mu_3\text{-}Se)_2(PPh_3)_4[Pt(cod)]\}^{2+}$ (**3**), and a byproduct $[Pt_3(\mu_3\text{-}Se)_2(PPh_3)_6]^{2+}$ (**4**) (eq 1).

$$\begin{aligned} &3Pt_2(\mu\text{-}Se)_2(PPh_3)_4\ (\mathbf{1}) + 3PtCl_2(cod) \rightarrow \\ &\quad \{Pt(\mu_3\text{-}Se)_2(PPh_3)_2[Pt(cod)]_2\}Cl_2\ (\mathbf{2})\ (m/z\ 742) + \\ &\quad \{Pt_2(\mu_3\text{-}Se)_2(PPh_3)_4[Pt(cod)]\}Cl_2\ (\mathbf{3})\ (m/z\ 950) + \\ &\quad\quad [Pt_3(\mu_3\text{-}Se)_2(PPh_3)_6]Cl_2\ (\mathbf{4})\ (m/z\ 1158) \end{aligned} \tag{1}$$

Although the exact formation mechanism is unclear, compound **3** is the obvious primary product, whereas **2** and **4** are secondary products formed from a scrambling process. An intermediate for **3** viz. $\{\mathbf{1}[PtCl(cod)]\}^+$ (m/z 1936) has been detected. Although **2** can arise from **3** through displacement of PPh_3 by cod, this is unlikely because there was no excess cod in the mixture, and such displacement would be inconsistent with the relative donor strength of the ligands. Indeed, when **3** was doped with free cod, there was no evidence for any significant formation of **2**, on the basis of ESMS or NMR data. The relative distribution of **2** and **3** is also not temperature or reaction duration sensitive. On the other hand, addition of $PtCl_2(cod)$ to a mixture of **1** and $PtCl_2(cod)$ tends to increase the formation of **2** (ESMS observation). This would support a Pt_4 intermediate such as $\{Pt_2(\mu_3\text{-}Se)_2(PPh_3)_4[PtCl(cod)]_2\}^{2+}$ which could conveniently give **2** by eliminating $PtCl_2(PPh_3)_2$. There is no other direct evidence that could verify this proposal. A similar form of scrambling has not been detected in the sulfur analogues. The shorter and stronger Pt−S bonds could provide better protection to the $\{Pt_2S_2\}$ core which would resist such attack.

The ^{31}P NMR analysis of this mixture at different stages gave only broad and complex peaks that do not render a

---

(12) Drew, D.; Doyle, J. R. *Inorg. Synth.* **1990**, *28*, 346.

(13) Ahmad, A.; Ainscough, E. W.; James, T. A.; Robinson, S. D. *J. Chem. Soc., Dalton Trans.* **1973**, 1148.

(14) Parshall, G. W. *Inorg. Synth.* **1970**, *12*, 27.

(15) Drew, D.; Doyle, J. R. *Inorg. Synth.* **1990**, *28*, 348.

(16) Burmeister, J. L.; Basolo, F. *Inorg. Chem.* **1964**, *3*, 1587.

(17) White, C.; Yates, A.; Maitlis, P. M. *Inorg. Synth.* **1992**, *29*, 229.

(18) Cinellu, M. A.; Zucca, A.; Stoccoro, S.; Minghetti, G.; Manassero, M.; Sansoni, M. *J. Chem. Soc., Dalton Trans.* **1995**, 2865.

Table 3. ESMS Data for Reactions between $[Pt_2(\mu\text{-}Se)_2(PPh_3)_4]$ (**1**) and Metal Substrates

combinations	cone voltage (V)	major ions (*m*/*z*, %)
1 + $PtCl_2(cod)$	20−40	$\{PtSe_2(PPh_3)_2[Pt(cod)]_2\}^{2+}$ (742, 43), $\{\mathbf{1}[Pt(cod)]\}^{2+}$ (950, 100)
	60	$\{PtSe_2(PPh_3)[Pt(cod)]_2\}^{2+}$ (611, 18), $\{PtSe_2(PPh_3)_2[Pt(cod)]_2\}^{2+}$ (742, 27), $\{(\mathbf{1} - PPh_3)[Pt(cod)]\}^{2+}$ (819, 53), $\{\mathbf{1}[Pt(cod)]\}^{2+}$ (950, 100)
	80	$\{PtSe_2(PPh_3)[Pt(cod)]_2\}^{2+}$ (611, 28), $\{(\mathbf{1} - 2PPh_3)[Pt(cod)]\}^{2+}$ (688, 83), $\{(\mathbf{1} - PPh_3)[Pt(cod)]\}^{2+}$ (819, 100), $\{\mathbf{1}[Pt(cod)]\}^{2+}$ (950, 3)
1 + *cis*-$PtCl_2[P(OPh)_3]_2$	20−60	$\{PtSe_2(PPh_3)_2\{Pt[P(OPh)_3]_2\}_2\}^{2+}$ (1255, 100)
	80	$\{PtSe_2(PPh_3)\{Pt[P(OPh)_3]_2\}_2\}^{2+}$ (1124, 100), $\{PtSe_2(PPh_3)_2\{Pt[P(OPh)_3]_2\}_2\}^{2+}$ (1255, 69)
1 + *cis*-$PtCl_2(PMe_3)_2$	20	$\{PtSe_2(PPh_3)_2[Pt(PMe_3)_2]_2\}^{2+}$ (786, 94), $\{\mathbf{1}[Pt(PMe_3)_2]\}^{2+}$ (972, 100), $\{\mathbf{1}[Pt(PMe_3)_2Cl]_2\}^{2+}$ (1181, 16)
	40	$\{PtSe_2(PPh_3)_2[Pt(PMe_3)_2]_2\}^{2+}$ (786, 100), $\{\mathbf{1}[Pt(PMe_3)_2]\}^{2+}$ (972, 90)
	60	$\{PtSe_2(PPh_3)[Pt(PMe_3)_2]_2\}^{2+}$ (655, 68), $\{PtSe_2(PPh_3)_2[Pt(PMe_3)_2]_2\}^{2+}$ (786, 100), $\{(\mathbf{1} - PPh_3)[Pt(PMe_3)_2]\}^{2+}$ (841, 75), $\{\mathbf{1}[Pt(PMe_3)_2]\}^{2+}$ (972, 65)
	80	$\{PtSe_2(PPh_3)[Pt(PMe_3)_2]_2\}^{2+}$ (655, 100), $\{PtSe_2(PPh_3)_2[Pt(PMe_3)_2]_2\}^{2+}$ (786, 20), $\{(\mathbf{1} - PPh_3)[Pt(PMe_3)_2]\}^{2+}$ (841, 71), $\{\mathbf{1}[Pt(PMe_3)_2]\}^{2+}$ (972, 10)
1 + $PdCl_2(cod)$	20−40	$\{\mathbf{1}[Pd(cod)]\}^{2+}$ (906, 100)
	60	$\{(\mathbf{1} - PPh_3)[Pd(cod)]\}^{2+}$ (775, 25), $[(\mathbf{1})Pd]^{2+}$ (852, 100), $\{\mathbf{1}[Pd(cod)]\}^{2+}$ (906, 93)
	80	$[(\mathbf{1} - PPh_3)Pd]^{2+}$ (721, 100), $\{(\mathbf{1} - PPh_3)[Pd(cod)]\}^{2+}$ (775, 23), $[(\mathbf{1})Pd]^{2+}$ (852, 61), $\{\mathbf{1}[Pd(cod)]\}^{2+}$ (906, 45)
1 + $PdCl_2(phen)$	20	$\{PtSe_2(PPh_3)_2[Pd(phen)]_2\}^{2+}$ (725, 40), $\{\mathbf{1}[Pd(phen)]\}^{2+}$ (942, 100)
	40	$\{PtSe_2(PPh_3)_2[Pd(phen)]_2\}^{2+}$ (725, 17), $\{\mathbf{1}[Pd(phen)]\}^{2+}$ (942, 100)
	60	$\{PtSe_2(PPh_3)_2[Pd(phen)]_2\}^{2+}$ (725, 13), $\{(\mathbf{1} - PPh_3)[Pd(phen)]\}^{2+}$ (811, 70), $\{\mathbf{1}[Pd(phen)]\}^{2+}$ (942, 100)
	80	$\{(\mathbf{1} - 2PPh_3)[Pd(phen)]\}^{2+}$ (680, 100), $\{PtSe_2(PPh_3)_2[Pd(phen)]_2\}^{2+}$ (725, 6), $\{(\mathbf{1} - PPh_3)[Pd(phen)]\}^{2+}$ (811, 91), $\{\mathbf{1}[Pd(phen)]\}^{2+}$ (942, 11)
1 + $[RhCl_2Cp^*]_2$	20−40	$\{PtSe_2(PPh_3)_2[Rh(Cp^*)]_2\}^{2+}$ (677, 52), $\{\mathbf{1}[Rh(Cp^*)]\}^{2+}$ (918, 100)
	60	$\{PtSe_2(PPh_3)_2[Rh(Cp^*)]_2\}^{2+}$ (677, 25), $\{(\mathbf{1} - PPh_3)[Rh(Cp^*)]\}^{2+}$ (787, 100), $\{\mathbf{1}[Rh(Cp^*)]\}^{2+}$ (918, 62)
	80	$\{(\mathbf{1} - 2PPh_3)[Rh(Cp^*)]\}^{2+}$ (656, 100), $\{(\mathbf{1} - PPh_3)[Rh(Cp^*)]\}^{2+}$ (787, 53), $\{\mathbf{1}[Rh(Cp^*)]\}^{2+}$ (918, 62)
1 + $AuCl_2(2\text{-}bzpy)$	20	$\{PtSe_2(PPh_3)_2[Au(2\text{-}bzpy)]_2\}^{2+}$ (805, 25), $\{\mathbf{1}[Au(2\text{-}bzpy)]\}^{2+}$ (982, 100)

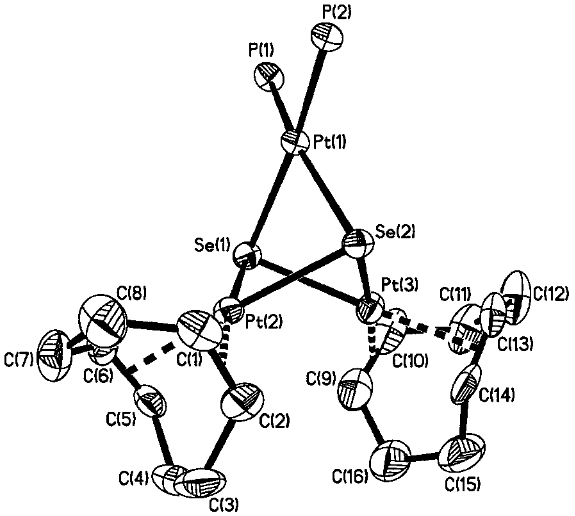

Figure 1. Molecular structure of the cation of $\{Pt(\mu_3\text{-}Se)_2(PPh_3)_2[Pt(cod)]_2\}\{PF_6\}_2$ **(2)**. The phenyl rings and PF_6 counteranions are omitted for clarity.

meaningful mechanistic description. When the reaction was carried out by Schlenk techniques at a synthetic scale, **2** and **3** were isolated in 55% and 28% yields. Their NMR (^{1}H and ^{31}P) spectra suggested that they are static at room temperature and that they differ by their cod/phosphine ligand ratio but gave no other useful structural information. Subsequent X-ray single-crystal crystallographic analysis revealed a trinuclear core, viz. $\{Pt(\mu_3\text{-}Se)_2(PPh_3)_2[Pt(cod)]_2\}\{PF_6\}_2$ (**2**) and $\{Pt_2(\mu_3\text{-}Se)_2(PPh_3)_4[Pt(cod)]\}\{PF_6\}_2$ (**3**). Their

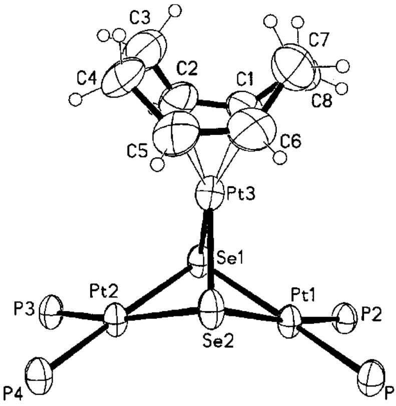

Figure 2. Molecular structure of the cation of $\{Pt_2(\mu_3\text{-}Se)_2(PPh_3)_4[Pt(cod)]\}\{PF_6\}_2$ **(3)**·$2.5CH_2Cl_2$·$3.5H_2O$. The dichloromethane and water of solvation, phenyl rings, and PF_6 counteranions are omitted for clarity.

selected bond lengths and angles are depicted in Table 1, and crystallographic data, in Table 2. The molecular structure of cationic **2** (Figure 1) shows a highly symmetrical trinuclear platinum aggregate consisting of two $\{Pt(cod)\}$ moieties connected to a $\{Pt(PPh_3)_2\}$ moiety through two selenium atoms. This was surprising as it signifies the disintegration of the $[Pt_2Se_2(PPh_3)_4]$ structural unit. Compound **2** is a rare example of a cod-rich system in low nuclearity clusters or aggregates. It is also surprising that this complex can be formed under such mild conditions from a phosphine-rich precursor. In our extensive study of the heterometallic sulfide analogues, such destruction has never been observed. Upon coordination of the $\{Pt_2Se_2(cod)_2\}$ moiety to $\{Pt(PPh_3)_2\}$, the Pt(2)−Se(1)⋯Se(2)−Pt(3) plane bends, thus making a dihedral angle of 111.6°. This is small compared to other reported examples (128°−133°),[5] which may reflect the lower steric demand of cod over (two) phosphines. Accordingly, it allows the P(1)−Pt(1)−P(2) angle to expand to 99.5°. The metalation by a unit of {Pt(cod)} on the Lewis basic selenide atoms on **1** afforded isolation of expected complex **3**. The molecular structure of cationic **3** (Figure 2) shows a highly symmetrical trinuclear platinum aggregate consisting of a {Pt(cod)} moiety resting on the {Pt_2Se_2} main core through the establishment of Se−Pt(cod) bonds. The replacement of a [Pt(cod)] moiety (in **2**) by sterically more demanding [$Pt(PPh_3)_2$] saw an increase in the dihedral angle [Pt(1)−Se(1)⋯Se(2)−Pt(2)] from 111.6° to 132.5°. The lower trans influence of cod (compared to PPh_3) selectively and consistently shortens, and presumably strengthens, the Pt−Se bonds trans to the cod [Pt−Se 2.4392(6)−2.4600(6) Å in **2** and 2.4283(10)−2.4305(11) Å in **3**] compared to those trans to the phosphine [2.4723(6)−2.4919(6) Å in **2** and 2.4607(10)−2.4744(9) Å in **3**].

Reaction of **1** with $PdCl_2$(cod) gave {**1**[Pd(cod)]}$^{2+}$ (*m*/*z* 906, 20 V) cleanly with no apparent scrambling. However, when **1** was mixed with other substrates, viz. [*cis*-$PtCl_2[P(OPh)_3]_2$, *cis*-$PtCl_2(PMe_3)_2$, $PdCl_2$(phen) (phen = 1,10-phenanthroline), [$RhCl_2Cp^*]_2$ (Cp* = η^5-C_5Me_5), and $AuCl_2$(2-bzpy) (2-bzpy = *C*,*N*-2-benzylpyridyl)], scrambling takes place. ESMS provides a unique and powerful means to observe such products (Table 3). At higher cone voltages (60−80 V), loss of PPh_3 ligands begins to take place. In general, products observed at lower voltages, the scrambled products included, are more likely to be reproduced at the synthetic level. Metal scrambling in this and other systems is sensitively dependent on the nature of metal and ligand (e.g., charge density and lability). We are still some distance away from predicting such behavior on the basis of structural and electronic data. However, at least with ESMS, we have at hand a diagnostic means to guide synthesis of such unusual and often unforeseen products.

Conclusions

By using ESMS, we have demonstrated a simple way to detect metal-scrambled products, and we have demonstrated that such spectrometric species can be synthesized and isolated. The coherence and consistency of the ESMS and structural data make this a powerful complementary approach in targeted synthesis. The resultant transformation of **1** to a mono cod and then to a bis cod system demonstrates that a Lewis basic and essentially saturated species can be transposed to one that is Lewis acidic and practically unsaturated. In this conversion, metal scrambling is no longer an undesirable process, as it yields an activated bis cod system that can serve as precursor for synthesis of extensive selenide arrays. For example, preliminary examination suggested that **2** can exchange with free dppe to give [$Pt(\mu_3\text{-}Se)_2(PPh_3)_2$-{Pt(dppe)}$_2$]$^{2+}$ (*m*/*z* 1032). This would provide a unique entry to mixed-phosphine, mixed-metal aggregates. We are currently looking for multiheterometallic networks using this spectrometrically directed synthetic approach.

Acknowledgment. The authors acknowledge the National University of Singapore (NUS) for support (Grant RP 3992749), and J.S.L.Y. thanks NUS for a research scholarship and for an attachment to University of Waikato. W.H. thanks the University of Waikato and the New Zealand Lottery Grants Board for financial assistance and Johnson Matthey plc for a generous loan of platinum. We thank G. K. Tan for her assistance in X-ray analysis.

Supporting Information Available: Crystallographic data in CIF format. This material is available free of charge via the Internet at http://pubs.acs.org.

IC010905T